The relative role of Amazonian and non-Amazonian fires in building up the aerosol optical depth in South America: A five year study (2005–2009)

ARTICLE *in* ATMOSPHERIC RESEARCH · MARCH 2013

Impact Factor: 2.42 · DOI: 10.1016/j.atmosres.2012.10.026

5 AUTHORS, INCLUDING:

Francesca Barnaba
Italian National Research Council
50 PUBLICATIONS **766** CITATIONS
SEE PROFILE

Federico Angelini
ENEA
42 PUBLICATIONS **302** CITATIONS
SEE PROFILE

Pablo Cremades
National Scientific and Technical Research …
7 PUBLICATIONS **5** CITATIONS
SEE PROFILE

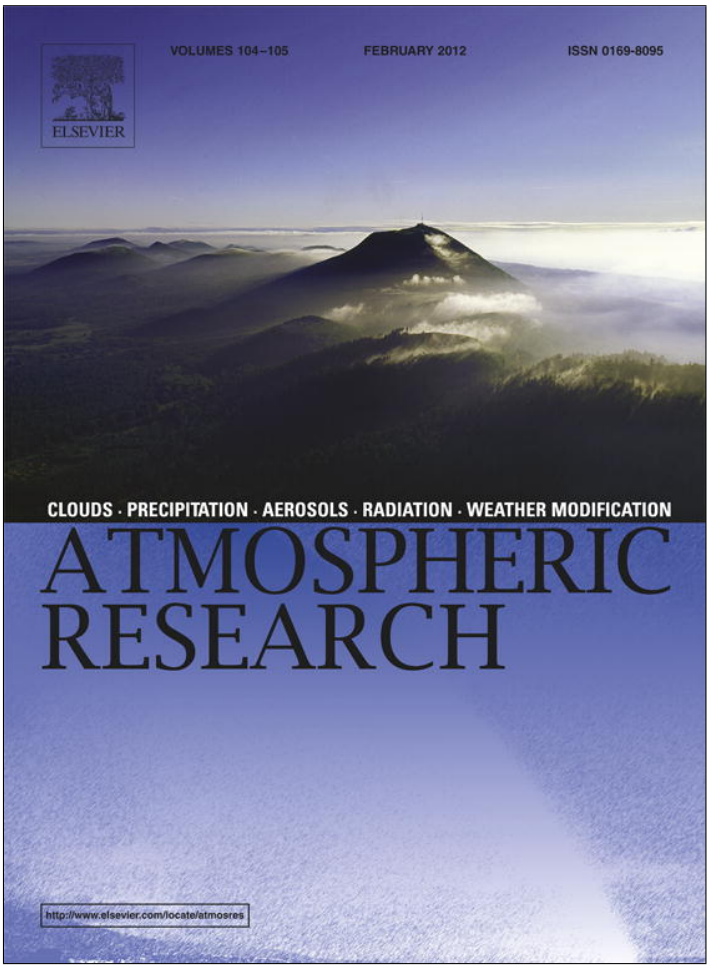

(This is a sample cover image for this issue. The actual cover is not yet available at this time.)

Atmospheric Research 122 (2013) 298–309

Contents lists available at SciVerse ScienceDirect

Atmospheric Research

journal homepage: www.elsevier.com/locate/atmos

The relative role of Amazonian and non-Amazonian fires in building up the aerosol optical depth in South America: A five year study (2005–2009)

Fernando Castro Videla [a], Francesca Barnaba [b,*], Federico Angelini [b], Pablo Cremades [a], Gian Paolo Gobbi [b]

[a] Universidad Tecnológica Nacional-Fac. Regional Mendoza, Mendoza, Argentina
[b] Istituto di Scienze dell'Atmosfera e del Clima-Consiglio Nazionale delle Ricerche (ISAC-CNR), Roma, Italy

ARTICLE INFO

Article history:
Received 5 July 2012
Received in revised form 25 October 2012
Accepted 26 October 2012
Available online 16 November 2012

Keywords:
Aerosol
Fires
Biomass burning
Long range transport
South America
MODIS

ABSTRACT

In South America (SA) biomass burning is the major source of atmospheric aerosols. Fires are mostly registered in the dry season (July–November) and are mainly concentrated in the Amazonia and Cerrado regions. Nonetheless, the growing systematic employment of fires for land clearing and pasture maintenance across the SA continent is introducing other, potentially significant, sources of BB aerosols. This study investigates the relative contributions of different SA biomass burning regions in building up the continental aerosol load. To this purpose, the SA continent is divided into four biomass burning source regions and their impact on the aerosol optical depth (AOD) is evaluated in eight different SA target domains. The dataset used includes multi-year (2005–2009) satellite observations of both aerosol and fires and model-based atmospheric trajectories. The methodology followed couples fire counts and atmospheric transport through the definition of a specific quantity, referred to as 'fire weighted residence time' (FWRT), which is used to assess the contribution of the four identified fire source regions to the continental aerosol load.

Results show that local fires play an important role in building up the regional aerosols load all over SA. Nevertheless, in some regions, contribution of BB aerosols transported from outside their boundaries is comparable to the local one. The major 'smoke exporter' regions are found to be the eastern Brazil and the Amazonia–Cerrado regions. In the dry season, due to the typical continental circulation pattern, the first is estimated to contribute to half of the AOD in Northern Amazonia, Southern Amazonia and Cerrado regions, while over 30% of the AOD in Paraguay and North Argentina derives from the Amazonia–Cerrado fires. Due to the presence of the inter-tropical convergence zone, which decouples wind circulation of the two hemispheres, regions north of the Equator (Venezuela, Guyana, Suriname) are found to receive almost no contribution to the local AOD from fires occurring in the nearby active regions of Amazonia and Caatinga. Similarly, Venezuela fires are shown not to impact the Northern Amazonia AOD. Finally, in excluding the continental fire driver of some AOD enhancements observed in the wet season, this study indirectly points to an important role of aerosol transoceanic transport from Africa.

1. Introduction

Biomass burning (BB) represents an important source of atmospheric aerosols and gases and is recognized to have an important role in regional and global climate changes (Forster et al., 2007). BB emissions reduce visibility and worsen air quality with enhanced risks for aviation transport and detrimental effects on human health (Martin et al., 2010). The South America (SA) continent is estimated to generate the world's highest biomass burning aerosol burden, about 50% of which is exported outside its boundaries, dominating much of the southern hemisphere (Koch et al., 2007). Wildfire emissions in

* Corresponding author at: ISAC-CNR, Via Fosso del Cavaliere 100, 00133, Roma, Italy.
E-mail address: f.barnaba@isac.cnr.it (F. Barnaba).

0169-8095/$ – see front matter © 2012 Elsevier B.V. All rights reserved.
http://dx.doi.org/10.1016/j.atmosres.2012.10.026

SA have been shown to markedly influence the regional and the global radiative balance both directly, by scattering and absorption processes (Artaxo et al., 2006; Procopio et al., 2004), and indirectly, by changing cloud microphysics and rainfall, and by suppressing cloud formation, with a significant influence on the overall water cycle (Andreae et al., 2004; Koren et al., 2004).

In South America, wildfires mainly occur during the dry season (July–November) and are mostly concentrated in the Amazon Forest and Cerrado regions (e.g., Martin et al., 2010; Schafer et al., 2008). A recent shift from forest to savanna/agricultural burning was documented for the Amazon basin, with a particularly intense fire activity at the edge of the forest frontier, where most of the land clearing activities occur (Ten Hoeve et al., 2012). In general, the growing systematic employment of fires for land clearing and pasture maintenance across the SA continent is introducing other, potentially significant sources of BB aerosols.

This study aims at quantifying the relative contribution of different SA biomass burning regions to the continental aerosol load in the recent years. The aerosol load is evaluated in terms of 'aerosol optical depth' (AOD), the column-integrated quantity typically derived from satellite which optically quantifies the aerosol burden in the atmosphere. As the aerosol spatial distribution over South America is distinctly influenced by the typical wind circulation pattern, the study combines multi-year (2005–2009) aerosol and fire data from satellite observations with forward trajectory modeling, following a procedure similar to that applied by Barnaba et al. (2011) to investigate the impact of fires over Europe.

Up to now, the number of studies investigating the role of regions other than Amazonia and Cerrado on the continental aerosol load is limited and relevant results still show some uncertainties. Mielnicki et al. (2005) analyzed space-based data of CO and AOD in eight different regions of South America and showed that the seasonality of AOD in each region does not depend uniquely on BB aerosols produced locally, as particles transported from other BB areas also play a non-negligible role. However, that study did not attempt to quantitatively disclose this twofold contribution in the eight zones investigated. Based on both ground-based and satellite data, Hoelzemann et al. (2009) revealed the predominant BB signal in SA to derive from emissions in the Amazon region and in the south of Brazil and Bolivia. Yet, both these studies could not discern quantitatively what is the origin of the increasing AOD observed in the southern part of SA during the BB season.

To understand the influence such large anthropogenic perturbations are having at the continental scale, it is also important to assess the background state of the atmosphere in the region. The Amazon forest has been generally considered a pristine environment in the wet season, with aerosols mainly originated by local biogenic sources (Martin et al., 2010). Some studies have however highlighted how, in this period of the year, the aerosol field and its variability in the Amazon region are largely affected by long-range transport of both desert dust and smoke from Africa. In fact, based on satellite observations, Kaufman et al. (2005) revealed that if from June to September transport of (almost pure) dust mainly occurs towards the Caribbean, from December to March a mixture of dust and biomass burning smoke from savannah fires in the Sahel (e.g., Roberts et al., 2009) is transported both above and below the equator, thus reaching the Amazon forest. This was confirmed by following dedicated campaigns, as the African Monsoon Multidimensional Analyses, AMMA, (Formenti et al., 2008), the Dust Outflow Deposition to the Ocean, DODO (Formenti et al., 2008), the SAharan Mineral dUst ExperiMent, SAMUM (Ansmann et al., 2009), and the Dust And Biomass Experiment, DABEX, (Johnson et al., 2008a,b) whose result clearly showed mixing of dust and biomass burning aerosols in the air masses flowing from Africa to Northern South America.

In fact, beside the major BB-driven enhancement of AOD in the dry season, a secondary AOD peak is often observed in the wet season over the northern SA. Schafer et al. (2008) attributed this AOD enhancement to dust transport from western Africa based on a 10-year climatology of aerosol optical properties in 15 sites of the Amazon region. Conversely, based on a 13-year time series of satellite data, Bevan et al. (2009) hypothesized this enhancement to be related to Venezuela fires. Our study will also provide some further insights into this aspect.

2. Datasets

This study is based on different, 5-year long (2005–2009) datasets. A first dataset includes daily forward trajectory computations employing the NOAA Hybrid Single-Particle Lagrangian Integrated Trajectory (HYSPLIT) model (Draxler and Hess, 1998). Two other main datasets are based on observations made by the MODIS sensor on board the NASA spacecraft Terra and include the MODIS-Terra aerosol optical depth (AOD) and the MODIS-Terra fire counts. Additionally, MODIS 'Fire Radiative Power' (FRP) data (Justice et al., 2006) were also used in sensitivity tests (Section 4.2) to evaluate the effects of a variable efficiency of different fire types in generating particles, which may change the ratio between the fire counts and the aerosols produced. FRP data used in this study come from the two MODIS instruments on board of the NASA Terra and Aqua platforms, these having overpass time of 10:30 am/10:30 pm LT and 1:30 pm/1:30 am LT, respectively. This double-platform dataset is used to evaluate possible effects on our results of the fire diurnal cycle.

A brief description of all these datasets is given below.

2.1. The forward trajectory simulations

A dataset of more than 100,000 forward trajectories from the HYSPLIT model is included in this study (Draxler and Hess, 1998). In particular, ten-days, 1 h-resolution, forward trajectories have been computed within the domain 15° N–55° S and 84° W–35° W. Trajectories are driven by the 1°-resolution NCEP analyses. We divide the domain in a regular 2.5°-resolution grid and start trajectories from those grid-cell centres where and when fires are detected. This resolution is chosen as a compromise between good spatial resolution of sources and acceptable computing time. A threshold of 1 fire-count/1000 km^2/day has been set for the single-trajectory computation. For the whole investigated period (2005–2009), a forward trajectory per day (at 10:30 LT) was computed. To ensure a boundary layer origin of the smoke and avoid ground effects, the starting altitude of the trajectories was set at 500 m above ground level (AGL). Some sensitivity tests were performed by changing the trajectories starting altitude within the first 1000 m and eliminating those trajectories for which the

500 m-starting altitude was above the model estimated 'atmospheric mixing layer' in the starting cell. Both tests showed minor changes (<10%) in the results presented in Section 4.

2.2. The MODIS AOD dataset

In this study we used the two MODIS-Terra aerosol products named 'Optical Depth Land and Ocean mean' and the 'Optical Depth Ratio Small Land and Ocean mean'. The first, here referred to as AOD, represents the integral of aerosol extinction over the atmospheric column and is retrieved in the visible region (at 550 nm). The second, here referred to as the fine fraction AOD (FFAOD), is the ratio of the small mode optical depth to the total AOD. The fine aerosol optical depth (fAOD) is then obtained by multiplying AOD by FFAOD. Both products have a spatial horizontal resolution of 1°×1° and an averaging time period of one calendar month. Detailed information on these aerosol products can be found in Hubanks et al. (2008) and Levy et al. (2009). These datasets are part of the MODIS Terra Collection 5, Level 3 (L3) gridded atmospheric data products. L3 MODIS products make use of aggregation and data quality weighting (Hubanks et al., 2008) through Level 2 data quality assurance (QA) bit flags. These range from QA = 0 ('No Confidence') to QA = 3 ('Very Good Confidence'). The AOD L3 product is linearly weighted with QA so that 'No Confidence' pixels are removed from the L3 statistics while 'Very Good Confidence' pixels have three times more weighting than the QA = 1 ('Marginal Confidence') ones.

The MODIS AOD product has been validated by Levy et al. (2010) through comparisons with coincident AERONET sun-photometer data (Holben et al., 1998). Based on long-term experience with the use of the MODIS data and interaction with user groups, the authors express their confidence in part of the data products and warn the users for over-confidence in other products such as those related to the aerosol size information. Within SA, poor comparisons of MODIS to 'ground-truth' AERONET data were mainly noted in the Patagonian region of Argentina (e.g., Trelew site, 43 S–65 W), which probably has a too bright surface for optimal use of the MODIS 'dark target' aerosol retrieval algorithm. Moreover, for some Brazilian sites as Alta Floresta (9 S–56 W, at the border of the Amazon forest) and Cuiaba (15 S–56 W, south in the Cerrado region, with a savanna-like vegetation), AOD values tend to be overestimated/underestimated in condition of high/low aerosol loads. These biases likely result from unrealistic assumptions in the MODIS retrieval of both aerosol models and surface reflectance. Levy et al. (2010) also warn on the use of the fAOD as a physical retrieval of aerosol particle size and consequently as a valid quantitative parameter. In this respect, it is however worth highlighting that in this work the fAOD parameter is only used 'qualitatively' as a proxy to reveal the presence of biomass burning aerosols. In fact, it is well known that BB particles are dominated by fine particles with an accumulation mode of 100–150 nm median diameter (Reid et al., 2005).

2.3. The MODIS fire datasets

Fire detection by satellite remote sensing is performed exploiting the strong emissions of mid-infrared radiation from fires. MODIS fire detection uses a contextual algorithm based on the brightness temperature derived from the 4 μm and 11 μm channels (Giglio et al., 2003). Fire counts used in this study are derived from the MODIS Terra Climate Modelling Grid (CMG) fire product, available through the NASA Earth Observations (NEO) portal (http://neo.sci.gsfc.nasa.gov). This is a gridded statistical summary of fire pixel information intended for use in regional and global modeling, with a spatial resolution of 0.5° for time periods of one calendar month. Detailed information about this and other fire products can be found in Justice et al. (2006).

In addition to 'fire counts', satellite sensors also measure the 'Fire Radiative Power' (FRP), i.e., the rate at which energy is emitted by a fire during the combustion (Kaufman et al., 1998; Giglio et al., 2003; Wooster et al., 2005). This can serve as an indicator of the aerosol (and gases) emission rate (e.g., Ichoku and Kaufman, 2005; Kaufman et al., 1998). In this study we use both MODIS-Terra and MODIS-Aqua monthly FRP data at 1° resolution available through the NASA-Giovanni web-based application (http://disc.sci.gsfc.nasa.gov/giovanni, developed by the NASA Goddard Earth Sciences Data and Information Services Center, e.g., Acker and Leptoukh, 2007).

3. Methods

3.1. Selection of SA biomass burning origin regions and target domains

To investigate the relative role of Amazonian and non-Amazonian sources on the South America AOD, four biomass burning 'origin regions' were defined over the continent (Fig. 1a). These are: the Venezuela–Colombia region (region A), the Amazonia–Cerrado region (region B), the Eastern Brazil–Caatinga region (region C), and the Paraguay–Argentina region (region D). The fire seasonality over the continent in the period addressed (2005–2009) is also shown in Fig. 1. In particular, Fig. 1a shows the monthly mean number of fires (fire counts/1000 km^2/day), while Fig. 1b shows the yearly cycle of the fire counts averaged over the four origin regions selected. These origin regions were chosen taking into account: 1) the typical fire seasonal behavior (Fig. 1), 2) the different land use over the continent (Fig. 2), and 3) the choice made by previous studies on the subject in order to facilitate comparison of our analysis with results available in the literature (e.g., Ichoku and Kaufman, 2005; Ichoku et al., 2008; Pereira et al., 2009).

Region A (Venezuela–Colombia, herein 'VenCol') comprises all fires produced from the equator to the north of the continent, more precisely in the Guiana forest region and in the Llanos savanna where farmers use fire for slash-and-burn practices as a way of obtaining fresh grass for their cattle and to clear fields for cultivation (Armenteras et al., 2005). Note that in this sector, differently from the other SA regions, fires mainly occur during the northern hemisphere dry season (i.e., December–May) (Fig. 1b).

Region B (Amazonia–Cerrado, herein 'AmazCerr') includes fires originated in the Amazonia tropical rain forest and in the Cerrado savanna region. The fire regime is strongly related to the southern hemisphere dry season (Fig. 1b), with maximum fire activity in August–September. In this region, the main human drivers of fires are land clearing for pasture, mechanized crop expansion and forest logging (Aragao et al., 2008).

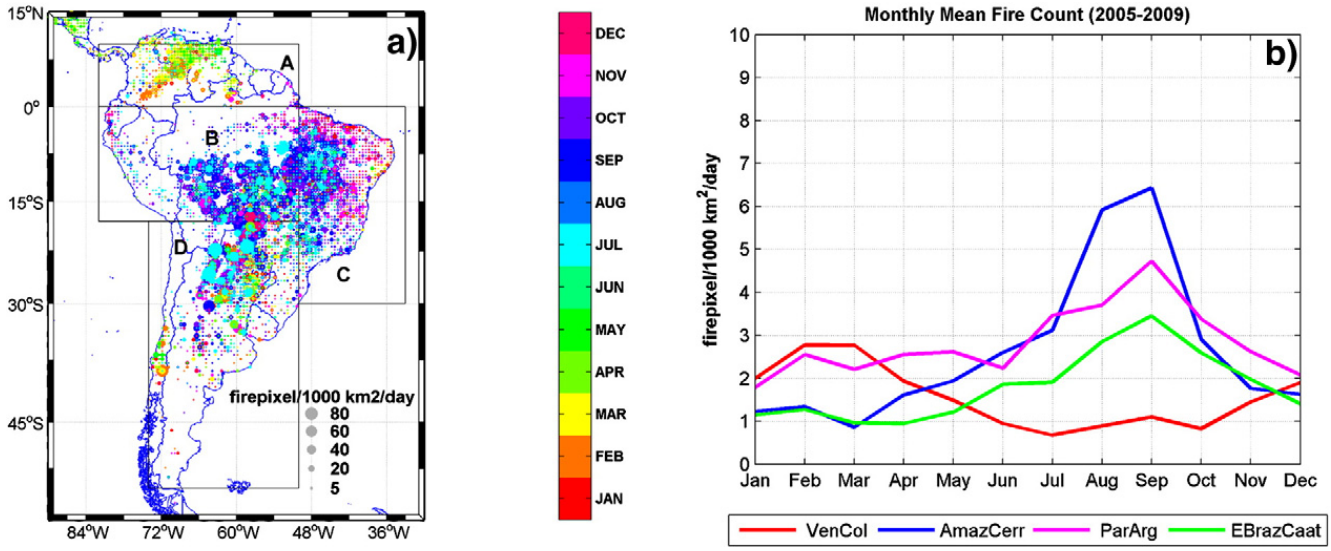

Fig. 1. a) Mean number of fires (circles) in the period 2005–2009 in each cell of 0.5°×0.5° and limits of the four selected origin regions (black lines): A) Venezuela and Colombia region (VenCol), B) Brazilian Amazon Tropical Rain Forest and Brazilian Cerrado (AmazCerr), C) Eastern Brazil–Caatinga biome (EBrazCaat) and D) Paraguay and Argentina region (ParArg). b) Mean seasonal variation of fires within each of the selected origin regions for the period 2005–2009.

Region C (Eastern Brazil–Caatinga, herein 'EBrazCaat') includes fires produced in the Brazilian Caatinga shrub lands and in the north-eastern part of the Cerrado region. The fire regime is similar to that of the Amazonia–Cerrado region but with a greater proportion of fires in October–November in the north and northeast of Brazil (Fig. 1) related with a delay in the onset of the dry season (Shafer et al., 2008).

Region D (Paraguay–Argentina, herein 'ParArg') includes the Paraguayan Chaco forest, the Pampas savanna and the grassland Argentinean regions. This region shares the July–November seasonality of fires with region C, but shows a higher number of fires in the first three months of the year (Fig. 1b). In the Pampas and the south of Chaco the expansion of the soybean crops and the sugar cane harvest can be pointed out as the main human driver of fires.

To evaluate the impact over the continent of the four BB origin regions identified above, eight different 'target domains' (TD) were also defined (Fig. 2). These TDs (numbered

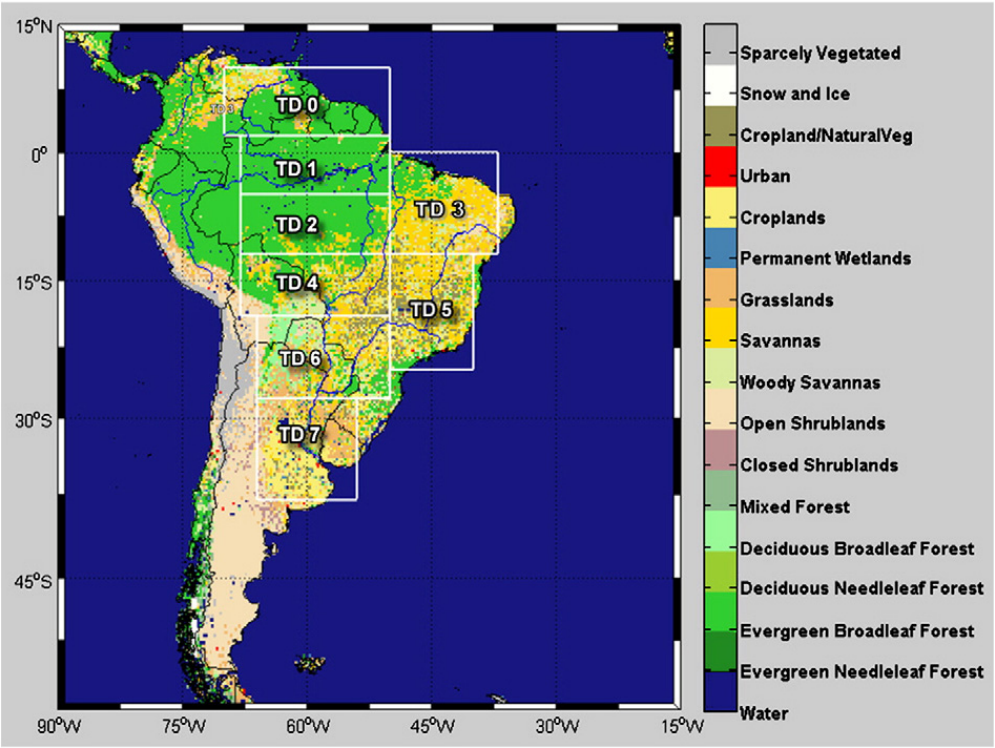

Fig. 2. Land use distribution (color code) and selected target domains (TD) (white lines) in South America. The TDs are numbered from 0 to 7 indicating respectively: 'Venezuela' (TD 0), 'Northern Amazonia' (TD 1), 'Southern Amazonia' (TD 2), 'Caatinga' (TD 3), 'Cerrado' (TD 4), 'Southeastern Brazil' (TD 5), 'Chaco' (TD 6), and 'Pampas' (TD 7). (For interpretation of the references to color in this figure legend, the reader is referred to the web version of the article.)

from 0 to 7) are: 'Venezuela', 'Northern Amazonia', 'Southern Amazonia', 'Caatinga', 'Cerrado', 'Southeastern Brazil', 'Chaco', and 'Pampas'. The target domains were chosen in order to keep a homogeneous land use within each sector (the surface albedo being one of the major uncertainties in the AOD product) and facilitate comparison with previous studies (e.g., Mielnicki et al., 2005; Shafer et al., 2008).

3.2. Coupling of the forward trajectories and fire counts: the FWRT parameter

A combination of aerosol sources and transport patterns is necessary to evaluate the relative contribution to the AOD of fires occurring in the different origin regions. To this purpose a specific quantity, referred to as the 'Fire-Weighted Residence Time' (FWRT), was calculated. The FWRT quantity couples the fire counts (used as a proxy of aerosol emissions) and the forward trajectories of air masses starting from the fire locations. For each month m and each 2.5° cell c of the whole domain considered (15° N–55° S and 84° W–35° W), the following quantity is computed:

$$\mathrm{FWRT}(m,c) = \sum_d \sum_n \left[\mathrm{F}_n \times \left(\sum_t \mathrm{e}^{-\mathrm{t}/\tau} \right) \right] \quad (1)$$

where n is the n^{th} cell of the domain, F_n is the monthly value of the fire counts in the n^{th} cell, t is the time (in hours) the forward trajectory originated in cell n keeps traveling over cell c. The exponential decay is applied to each trajectory in order to simulate the dry removal of aerosols along the trajectory path (a time constant value of $\tau = 5$ days, i.e. 120 h, was chosen according to the studies of Ahmed et al. (2004) and Papastefanou (2006). The aerosol wet deposition is included by stopping the trajectory computation when the cumulative precipitation derived by the model was above the threshold of 10 mm. Being the trajectories computed on a daily basis, the sum over the days d within the month m is computed to achieve the monthly statistics. Examples of the monthly FWRT fields (January and October 2009) derived by Eq. (1) are shown in Fig. 3 (panels 3a and 3b, respectively), which illustrates the FWRT ability to couple the fire-related aerosol sources to the atmospheric transport.

The FWRT fields were then integrated over each target domain, TD, obtaining for each of these, the following quantity:

$$\mathrm{FWRT}(m,\mathrm{TD}) = 1/\mathrm{C} \sum_{c \in TD} [\mathrm{FWRT}(m,c)] \quad (2)$$

i.e., the integral of the FWRT field over those cells c belonging to the target domain TD. As the eight target domains have different sizes, to make the FWRT values over the TDs comparable, a normalization to the total number of cells in the TD (factor 1/C) is applied in Eq. (2). A graphical scheme of this procedure, can be found in Barnaba et al. (2011) who applied a similar approach to evaluate the role of wildfires over Europe.

Main shortcomings embedded in the FWRT-based methodology include: 1) the inability of the FWRT parameter to reproduce the accumulation of aerosols in the atmosphere (which often translates into a time shift in the appearance and disappearance of the FWRT signal in comparison to that of the AOD), 2) the variable efficiency of fires in emitting aerosol particles, which may change the ratio between the fire counts and the aerosol produced (assumed as 1 in this study) and 3) the diurnal cycle of fires which could in principle bias the derived link between the AOD and fire-related fields.

These points are discussed in Section 4, with points 2) and 3) specifically addressed through sensitivity tests described in Section 4.2.

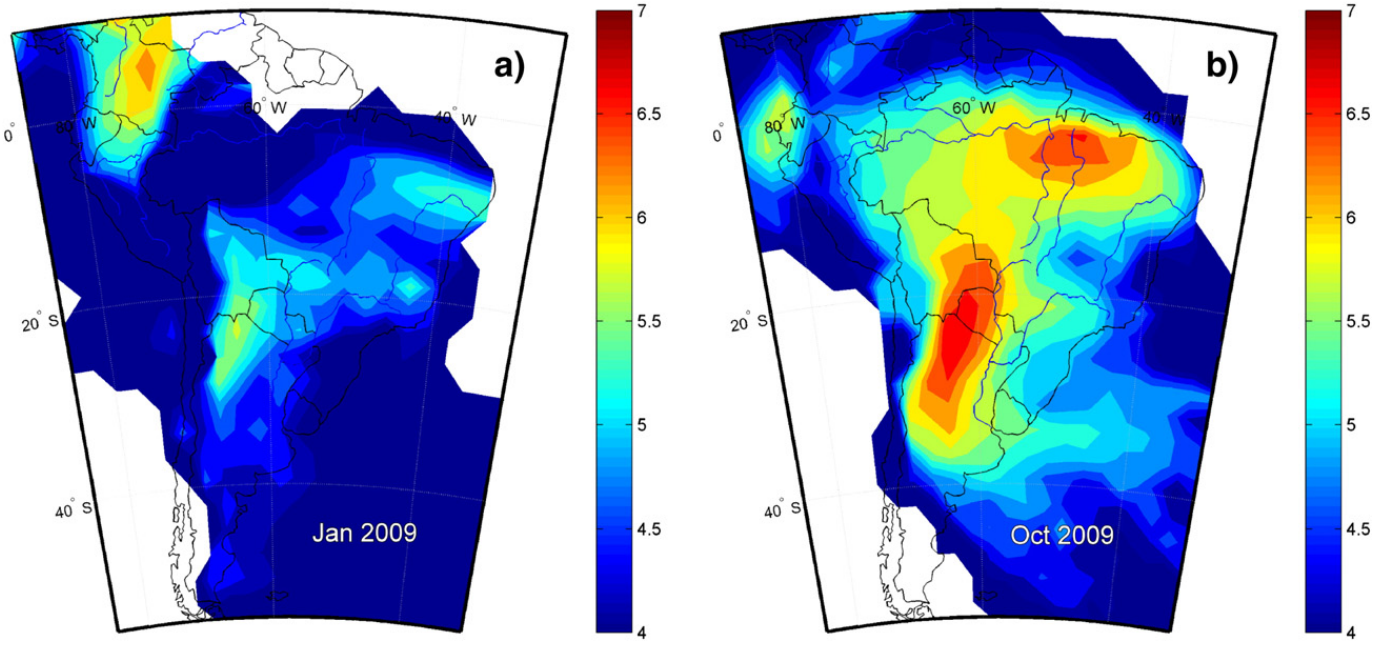

Fig. 3. FWRT field (logarithmic scale) as obtained for the months of a) January 2009 and b) October 2009. Blank regions are those where log(FWRT)<4.

4. Results and discussion

The monthly statistics (mean and standard deviation, s.d., over the period 2005–2009) of the AOD and fAOD satellite retrievals as well as of the FWRT parameter obtained as described in Eq. (2) are summarized in Fig. 4 for each target domain (Fig. 4a to h). In TDs 2, 4 and 6 (Southern Amazonia, Cerrado, and Chaco, respectively) the seasonal behavior of

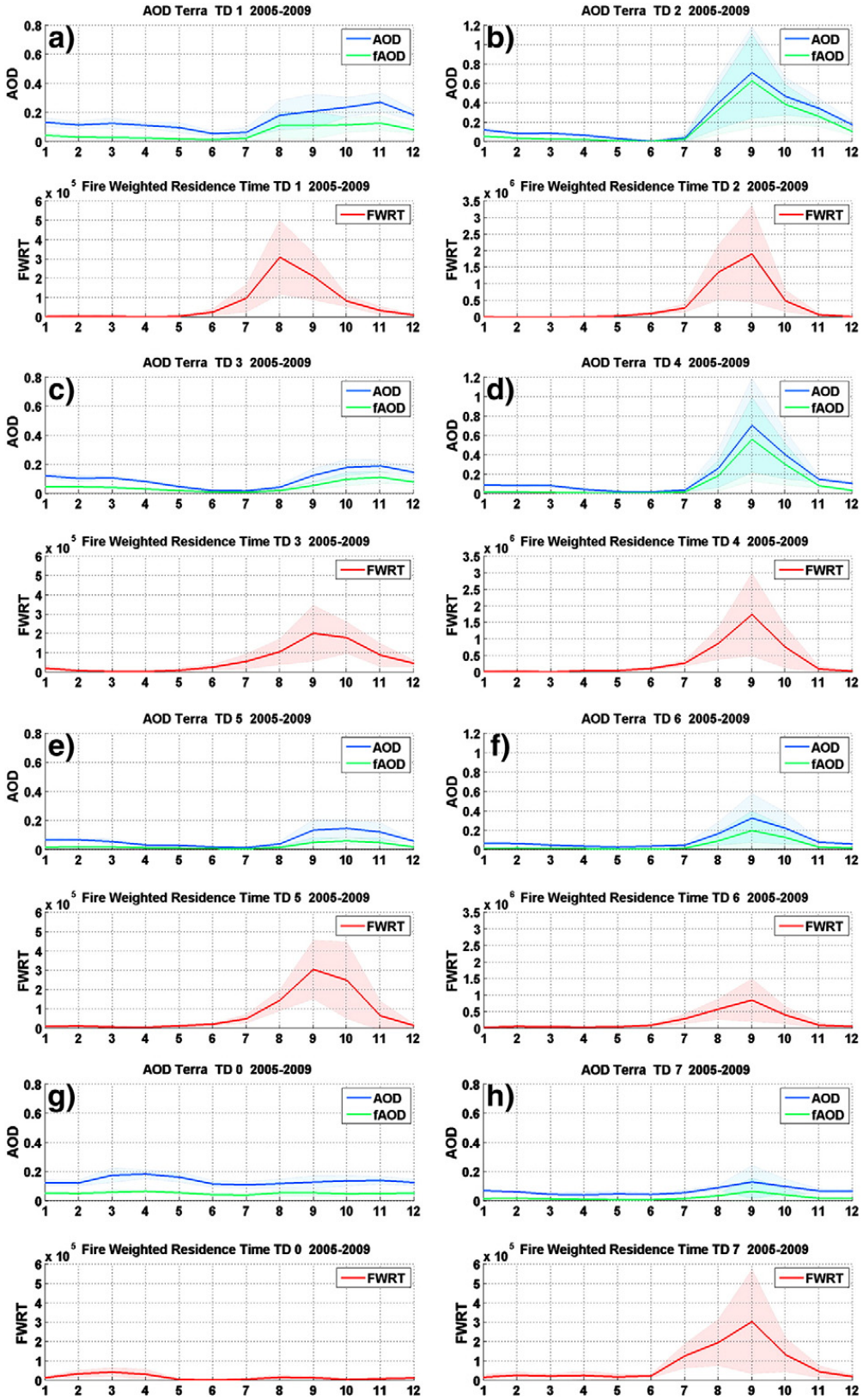

Fig. 4. Monthly mean FWRT, AOD and fAOD during the period 2005–2009 for all target domains. Shaded areas represent ±1 standard deviation from the monthly mean values. (For interpretation of the references to color in this figure legend, the reader is referred to the web version of the article.)

AOD and fAOD (blue and green curves) is very similar (Fig. 4b, d, f), revealing the strong biomass burning influence in the period July–November, fine mode aerosols dominating the AOD. In these TDs, September is the peak month, with mean values of AOD (fAOD) decreasing from 0.7 to 0.3 (0.6 to 0.2) moving from north (TD 2) to south (TD 6). Note that the BB aerosols signature is revealed not only by the mean AOD trace, but also by its associated standard deviation (s. d., shaded area in Fig. 4). In fact, the fire activity exhibits a significant inter-annual variability translating into a high standard deviation which conversely keeps low out of the burning season when a mean AOD of about 0.1 can be observed (minimum in May–June). These results are very similar to the AOD seasonal patterns observed over these regions by ground-based remote sensing (Shafer et al., 2008).

The biomass burning driver of the observed AOD (and fAOD) peak in these three TDs is confirmed by the yearly variability of the FWRT parameter. In fact, the FWRT cycle very closely follows the AOD (and fAOD) one, although an early rise of the FWRT with respect to the AOD is observed in June. This time shift is likely related to the fact that aerosols produced by fires (either via direct injection and secondary processes) tend to accumulate in the atmosphere producing some delay in the AOD rise. A similar reason could explain the faster decrease of FWRT in the months following the biomass burning peak (particularly in TD 2) as, once stopped the aerosol emissions, it takes a while to re-establish 'background' AOD conditions. As expected, due to the high number of fires registered (e.g., Fig. 1) and their position in the continental wind circulation path, these three TDs are associated to AOD and FWRT values both higher than those characterizing all the other target domains addressed in this study (note the different FWRT scales in Fig. 4b, d, and f with respect to the others).

The AOD peak in the period July–December is still visible in target domains 1, 3 and 5 (Northern Amazonia, Caatinga, Southeastern Brazil, Fig. 4a, c, and e, respectively), but in this case the maximum AOD values (about 0.2) are shifted to October–November. Differently from the previous cases (TDs 2, 4, 6), this AOD behavior is only partially reproduced by the FWRT parameter (our BB indicator). In the TDs closer to the coast (TDs 3 and 5), the FWRT keeps showing its maximum on September, although with a smoother decrease from October to November with respect to the central SA target domains (TDs 2, 4, 6). This indicates that, in this period of the year, fires are still contributing to the AOD, but also points to an important additional aerosol source different from the continental BB one. This is even more evident in TD 1, showing the highest AOD in November, which is clearly not related to continental biomass burning. Note also that this additional source keeps playing a relevant role in TDs 1, 3, and (partially) 5, until at least the first months of the year. Episodic transport of dust (Ben-Ami et al., 2010; Koren et al., 2006; Formenti et al., 2001) or smoke (Freitas et al., 2005) plumes from Africa to SA has been documented, but the results in Fig. 4 (similar contribution of fine and coarse particles to the AOD) mainly point to a mixed smoke/dust aerosol transport towards SA, in agreement with previous findings (e.g., Ansmann et al., 2009; Kaufman et al., 2005; Shafer et al., 2008). In the first months of the year, this double African source likely makes most of the AOD in the northern SA, with AOD values up to about 0.15 in the Northern Amazon region (TD 1).

To the south of the continent, the AOD and fine AOD patterns are similar to the ones observed in TDs 2, 4 and 6, but with markedly reduced absolute values (maximum AOD of about 0.1 in central Argentina (TD 7, i.e., Pampa)). September is still the month in which AOD and its fine aerosol portion peak, with a typical signal of the biomass burning driver from July to November (Fig. 4h). In the first three months of the year a small increase in AOD and fAOD is observed, but, as opposite to the northern part of the continent, in this case, this AOD increase is likely related to local aerosols from summer fires in Northern Argentina and Paraguay (note the low, but non-null FWRT levels in Fig. 4h, as further detailed in Section 4.1).

The TD 0 (Venezuela) shows a different seasonal behavior in AOD and fAOD with respect to the other target domains addressed, with maxima AOD (fAOD) of about 0.2 (0.065) in March–April (Fig. 4g). This uncoupling of TD 0 from those target domains below the equator is due to a different local fire regime (Fig. 1) and to the atmospheric general circulation pattern which translates into a minor exchange of air masses between the two hemispheres. The FWRT parameter is able to follow the AOD behavior indicating a non-negligible impact of fire-related aerosols to the TD0 AOD.

Still, in this TD the coarse fraction represents more than 50% of the total AOD, thus suggesting that aerosol transport from Africa (either dust and aged biomass burning) also plays a role in defining AOD seasonal behavior in the SA equatorial region.

The general ability of the FWRT-based methodology to identify the contribution of biomass burning on the SA aerosol load is evaluated through correlations between the monthly FWRT data and the relevant monthly mean fAOD. Results for the period 2005–2009 are summarized in Table 1 for each target domain. As expected, the correlation is relatively good ($R>0.7$) and statistically significant ($p \ll 10^{-9}$) for those TDs in which the fAOD is mainly driven by the BB emissions and/or its transport (i.e., TD = 2, 4, 5, 6, 7). The correlation is conversely low ($R<0.6$) in the northernmost regions (TD = 0, 1 and 3) where, as discussed, local BB is not the only, nor the main, aerosol source.

Table 1
Correlation coefficients (R) and correlation statistical significance (p) between the monthly MODIS fAOD and the corresponding FWRT and the RWRT values over the eight target domains (Fig. 3).

Target domain	fAOD–FWRT		fAOD–RWRT	
	R	p	R	p
0 (Venezuela)	0.27	0.04	0.32	0.013
1 (Northern Amazonia)	0.61	1×10^{-7}	0.55	6×10^{-6}
2 (Southern Amazonia)	0.88	5×10^{-21}	0.77	6×10^{-13}
3 (Caatinga)	0.48	1×10^{-4}	0.54	7×10^{-6}
4 (Cerrado)	0.94	6×10^{-28}	0.83	9×10^{-17}
5 (Southeastern Brazil)	0.70	3×10^{-10}	0.67	3×10^{-9}
6 (Chaco)	0.92	5×10^{-25}	0.79	7×10^{-14}
7 (Pampa)	0.86	2×10^{-18}	0.68	1×10^{-9}

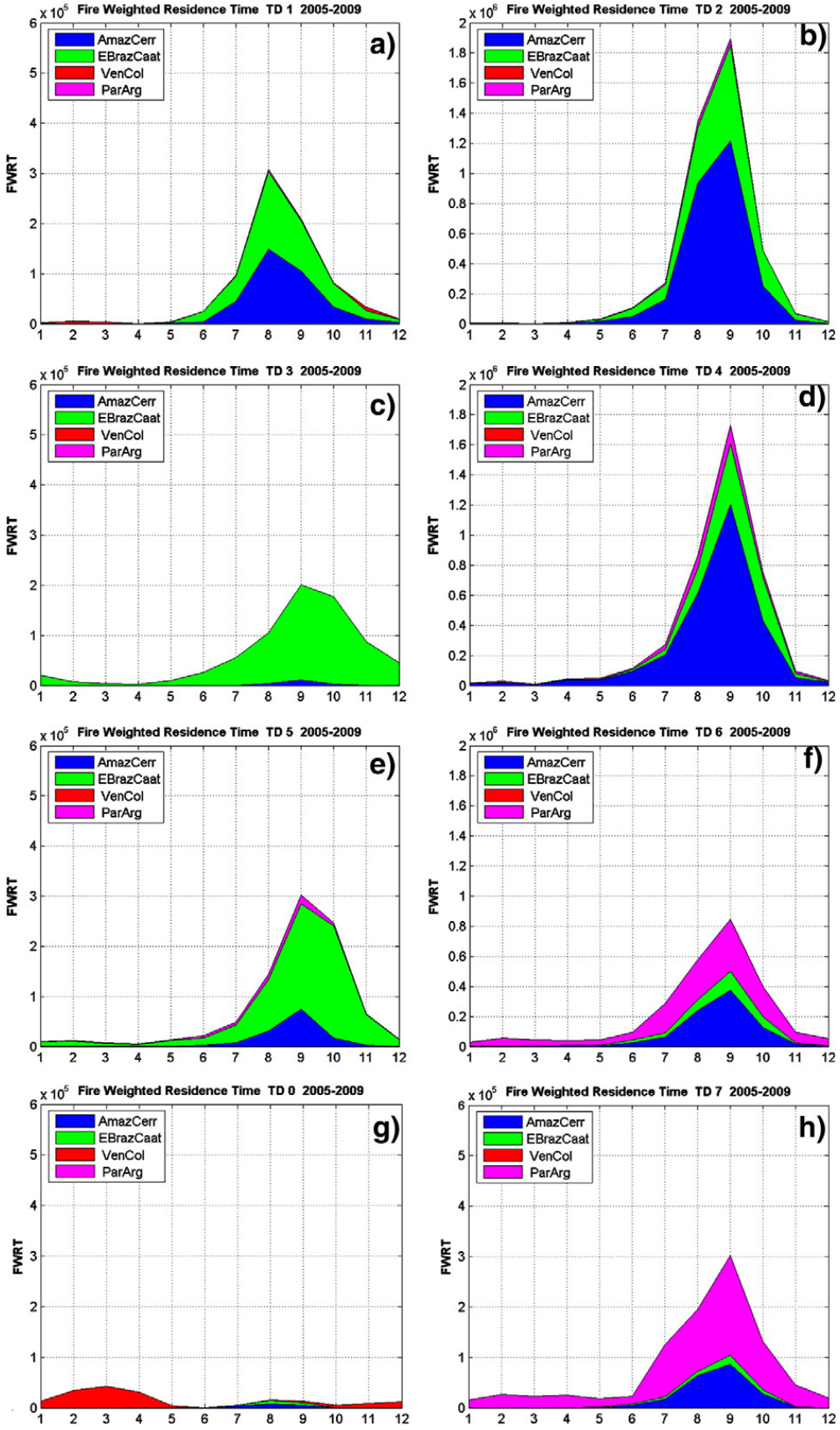

Fig. 5. Monthly FWRT fields in each target domain (TD) and relative contribution of fires in the four different origin regions (see legend). Note that panels b), d) and f) have a different y-axis scale.

4.1. Origin region contributions to the fire-related SA aerosol load

Continental biomass burning is the main factor building the AOD over most of SA, but this does not answer the question on which fires are the ones contributing most in every TD. Certainly, local fires are of great importance in every TD but, given the different fire regimes among the SA regions and the typical SA circulation pattern, in some TDs long-range aerosol transport from outside their boundaries could even exceed the local effects. To our knowledge, quantitative estimates of the monthly-resolved contribution of different continental fire areas on the SA aerosol load are not available in the literature. The FWRT parameter set up in this study helps in addressing this issue. In particular, for each month and TD, the contribution of each origin region (Fig. 1a) to the total FWRT value given in Fig. 4 has been computed and the results are reported in Fig. 5. The relative (percentage) contribution of the four origin regions (A, B, C, and D) to the monthly-resolved FWRT values is also summarized in Tables provided in the supplementary material (Tables S1A, S1B, S1C, S1D). Fig. 5 shows that in the Northern Amazonia target domain (TD 1), local fires (origin region B — 'AmazCerr') contribute to a maximum of 50% (September) of the total FWRT, but, due to almost constant low level easterly winds, a comparable contribution (48%) is given by fires occurring in the northeast of Brazil (origin region C — 'EBrazCaat') during the whole dry season. Only during the summer months, emissions and transport of fires located north of the equator (origin region A — 'VenCol') are detectable on the low TD1 FWRT signal (in March this contribution exceeds 90% of the total FWRT, Table S1A). Nevertheless, as previously commented, such a minor absolute FWRT signal does not explain the rather high values of AOD (50% of which made by coarse particles) observed between November and April (see Fig. 4a) and indirectly points to long-range aerosol transport from Africa (mixed desert dust and biomass burning particles).

In TDs 2 and 4 (which include the southern border of the Amazon forest, Cerrado and Bolivian Amazon), where the largest amount of SA fires is produced, the FWRT is mostly build up by local fires (origin region B — 'AmazCerr') all over the year. However, the contribution to the FWRT of fires located northeast of Brazil (origin region C — 'EBrazCaat') is again not trivial. In October, when the absolute FWRT is still high, it reaches up to about 50% and 40% in TD 2 and TD 4, respectively, suggesting similar contribution percentages to the AOD.

In the target domains 3 and 5, located within the origin region C, local fires markedly dominate the FWRT signal. This effect is more evident in TD 3 (almost 100% of the FWRT due to fires in the 'EBrazCaat' region) since the easterly circulation is stronger close to the equator than at higher latitudes. In fact, at higher latitudes the presence of the South Atlantic subtropical high (SASH) and cold fronts arriving from the south force easterly winds to turn southeast, determining the main path of smoke transport to the Atlantic Ocean. This circulation also transports smoke produced in the 'AmazCerr' and 'ParArg' regions to the east, the first contributing up to 25% of the FWRT in TD 5 during the southern hemisphere winter. The flow of air masses over SA produces a net transfer of smoke emissions from the Amazon region to the south of the continent in a low-level jet structure (Longo et al., 2006; Freitas et al., 2005; Otero et al., 2009). This transfer of smoke can be observed and quantified in the origin-region-resolved FWRT values obtained for TD 6 and TD 7. During the period June–October, in these southernmost TDs the contribution of fires from the origin region B ('AmazCerr') keeps significant, reaching maximum values in August–September (about 40% in TD 6 and 30% in TD 7). Conversely, in the same June–October period, the contribution of the origin region C ('EBrazCaat') to these TDs keeps lower than about 20% and 10%, respectively. Out of this period, the FWRT values in both these TDs are almost entirely built up by fires in Paraguay and North-central Argentina (origin region D). The latter origin region has conversely a minor impact on all the other TDs (below 15% in the period Jul–Nov), the highest contributions being mainly related to deviations in the predominant circulation pattern.

North of the equator, in TD 0, there is a marginal contribution of non-local fires in the buildup of the FWRT field because, as already mentioned, the wind circulation is uncoupled from regions south of the equator. In fact, during the SA burning season the FWRT contribution due to transport from the origin regions B and C exceeds 50%, but the absolute value of FWRT is almost negligible. Consequently, FWRT in TD 0 shows a completely different yearly pattern with respect to those already addressed, as mainly influenced by local fires (origin region A — 'VenCol') maximizing in February–April (Fig. 1).

4.2. Sensitivity tests: fire efficiency and diurnal cycle

As mentioned, a variable efficiency of different fire types in generating particles may change the ratio between the fire counts and the aerosols produced, thus potentially altering the findings reported above.

Specific sensitivity tests were then performed using a metric different from the fire counts to weight the fires ability to generate particles within the FWRT-based methodology. In particular, we weighted the forward trajectory-densities by the MODIS-Terra fire radiative power (FRP). In fact, being the FRP related to the fire behaviour and the mass of fuel consumed (Giglio et al., 2003), it is often preferred to the fire counts to estimate and characterize the biomass burning emissions (Ichoku and Kaufman, 2005; Ichoku et al., 2008; Pereira et al., 2009).

Similarly to the FWRT, we then derived a further quantity, referred to as Radiative-power Weighted Residence Time (RWRT). In this case, the monthly fire count value of each n^{th} cell of the domain, F_n in Eq. (1), is replaced by the relevant monthly mean FRP_n (MW or Mjs^{-1}).

Results of the overall correlations between fAOD and RWRT, are also reported in Table 1. The correlation coefficients obtained are generally lower than those derived with the FWRT and the latter was therefore preferred in this study to quantify the relative contribution of different SA biomass burning regions to the continental aerosol load. Note however that results very close to those derived with the FWRT are obtained with the RWRT field (see Fig. S1 and Tables S2A, S2b, S2C, and S2B provided in the supplementary material), and all the findings reported in Section 4.1 are substantially confirmed by this alternative methodology. This is because, following Eqs. (1) and (2), our approach is almost insensitive to the absolute value of the fire-related field used (FWRT or RWRT in

this case), but extremely dependent on both its timing (i.e., monthly variability) and on the relative (metric-dependent) weight of fires in the different origin regions.

For reasons similar to those described above, the use of MODIS-Terra rather than MODIS-Aqua fires data is not expected to largely bias our results. In fact, over South America fire activity maximizes in the early afternoon (e.g., Prins et al., 1998; Giglio et al., 2006), and therefore fire detections from the MODIS-Aqua instrument are generally higher than the mid morning ones from Terra. Based on fire pixel counts over South America from July 2002 to June 2005, Giglio et al. (2006) quantify the Aqua fire counts as a factor of 2 higher than the Terra ones. A similar ratio (1.81 ± 0.12) has been obtained by Mu et al. (2011) for the period 2003–2009. Nevertheless, Giglio et al. (2006) also show that seasonality of fires as depicted by Terra and Aqua is basically the same. As said, in our study time series showing different absolute numbers of fire-related metrics (e.g., fire counts and/or FRP) but with a similar monthly pattern would simply translate into re-scaled values of the regional FWRT (and/or RWRT) field. This means that both the FWRT (RWRT) seasonal pattern (Fig. 4) and the relative contribution to it of the four origin regions (Fig. 5 and Fig. S1) would be similar, thus keeping the study results unaltered.

This was verified computing the equivalent of the RWRT field described above using MODIS-Aqua rather than MODIS-Terra FRP data. Results of this test (summarized in Fig. S2 and Tables S3A, S3b, S3C, and S3B provided in the supplementary material) basically confirm all the quantitative results presented in Section 4.1. The only difference of the RWRT-based results (both from Terra and Aqua data) is a reduced role of the origin region B in TD 6 and TD 7 compensated by an increased weight of local fires (i.e. of the origin region D) in these southernmost target domains (see Tables S2B, S3B, S2D, and S3D).

As a final remark, also note that our preferential choice of MODIS-Terra data was related to the fact that, due to a more likely presence of clouds in the afternoon, the statistics of aerosol data as derived from Aqua is generally lower than the Terra one (we estimated that, over the whole South America and in the 2005–2009 period considered, the cloud fraction at the Aqua overpass is about 25% higher than that at the Terra overpass time).

5. Summary and conclusions

In this work the relative contribution of biomass burning aerosols from different SA regions in building up the continental AOD has been investigated and quantified based on long term (2005–2009) aerosols and fire satellite data (MODIS Terra) coupled to forward trajectory modeling. A specific quantity, the Fire Weighted Residence Time (FWRT), has been computed to couple the satellite fire counts (used as a proxy of the biomass burning emissions) with the atmospheric transport (simulated through forward trajectories from the fire locations).

High correlations between the computed monthly FWRT data and the relevant fine aerosol optical depth (fAOD) over eight Target Domains in SA demonstrated the FWRT ability to reveal the biomass burning fingerprints on the SA fAOD. Exceptions only occurred in the northeastern part of the continent where, as well documented in the literature, intercontinental aerosol transport of dust and smoke from Africa also significantly contributes to build up the local aerosol load (a signal that, for its specific nature, cannot be detectable by our FWRT-based method). Sensitivity tests employing satellite fire radiative power data rather than fire counts as a proxy for fire aerosol emissions show minor changes in the results, thus reinforcing the validity of our findings.

Overall, main results of this study could be summarized as follows:

1) Depending on the occurrence of the dry season, fires have a different seasonality over SA. In the northern hemisphere fires show their maximum occurrence around March and consequently the fAOD also peaks in this period. In the central part of Brazil, Bolivia, Paraguay and Argentina, the peak of fires is observed around September producing a great signal in fAOD that contrasts with the low aerosol load present in the first semester. In the northeastern part of Brazil the dry season is delayed by about a month and the peak of fires and fAOD is shifted to October–November. This zone is subject to an all-year-long influence of aerosol transport from African sources (both desert dust and biomass burning).
2) It is clear that local fires play an important role in building up the regional aerosol load all over SA. However, being aware of the large amounts of aerosol produced by biomass burning, the long-range transport of smoke within the continent is also shown to significantly contribute in regions far from the source one.
3) In the eastern part of Brazil (target domains 3 and 5) the fAOD is almost completely dominated by local fires and the region acts as a 'smoke exporter'. In fact, due to the trade winds blowing toward the continent year-round, the contribution to the fAOD of fires occurring in this part of the continent (the 'EBrazCaat' region) reaches over 40% in the target domains of Southern Amazonia (TD2) and Cerrado (TD4).
4) As showed by other authors (Freitas et al., 2005; Longo et al., 2006; Otero et al., 2009), there is also a net transport of smoke to the south of the continent from the Amazonia and Cerrado regions. The presence of the SASH and the Andes barrier forces easterly winds to turn south and smoke is transported to Paraguay and Argentina down to 35–40° latitude south (TDs 6 and 7). In these regions, we estimate a non-local contribution to the fine AOD during the biomass burning season higher than 30%.
5) In Northern Amazonia, the FWRT analysis suggests an almost equal contribution to the aerosol load of local fires and fires occurring in the nearby region of the Eastern Brazil–Caatinga, revealing conversely a negligible contribution from fires located north of the equator. This refutes the hypothesis of Bevan et al. (2009) that the Amazonia AOD peak observed in March is due to smoke transport from Venezuela fires. Rather, this result, coupled to the observation of a significant contribution of coarse particles to the AOD in the wet season, points to a major role of intercontinental transport of African dust.
6) North of the equator biomass burning contributions due to transport from other SA regions is almost negligible because of the uncoupled wind circulation from regions south of the equator.
7) Sporadic deviations from the typical wind circulation pattern (e.g., polar fronts heading north) produce some

transport of fire emissions in Argentina and Paraguay to the central part of Brazil, quantified in about 10% of the fine AOD in the Brazilian Cerrado region.

Acknowledgments

The authors gratefully acknowledge the MODIS mission scientists and associated NASA personnel for the production of the data used in this research effort and the NOAA Air Resources Laboratory (ARL) for the provision of the HYSPLIT transport and dispersion model used in this publication. MODIS fire count data used in this study were obtained from the NEO web portal as part of the NASA EOS Project Science Office. MODIS FRP data were produced with the Giovanni online data system (NASA GES DISC) under the NASA Northern Eurasia Earth Science Partnership Initiative.

F. C. was supported by the Italian Ministry of Foreign Affairs through its 2009/2010 scholarship program for foreign students.

Appendix A. Supplementary data

Supplementary data to this article can be found online at http://dx.doi.org/10.1016/j.atmosres.2012.10.026.

References

Acker, J.G., Leptoukh, G., 2007. Online analysis enhances use of NASA earth science data. EOS Trans. Am. Geophys. Union 88 (2), 14–17.

Ahmed, A.A., Mohamed, A., Ali, A.E., Barakat, A., Abd El-Hady, M., El-Hussein, A., 2004. Seasonal variations of aerosol residence time in the lower atmospheric boundary layer. J. Environ. Radioact. 77, 275–283.

Andreae, M.O., Rosenfeld, D., Artaxo, P., Costa, A.A., Frank, G.P., Longo, K.M., Silva-Dias, M.A.F., 2004. Smoking rain clouds over the Amazon. Science 303 (5662), 1337–1342.

Ansmann, A., Baars, H., Tesche, M., Müller, D., Althausen, D., Engelmann, R., Pauliquevis, T., Artaxo, P., 2009. Dust and smoke transport from Africa to South America: Lidar profiling over Cape Verde and the Amazon rainforest. Geophys. Res. Lett. 36, L11802. http://dx.doi.org/10.1029/2009GL037923.

Aragao, L.E., Malhi, Y., Barbier, N., Lima, A., Shimabukuro, Y., Anderson, L., Saatchi, S., 2008. Interactions between rainfall, deforestation and fires during recent years in the Brazilian Amazonia. Philos. Trans. R. Soc. B Biol. Sci. 363, 1779–1785.

Armenteras, D., Romero, M., Galindo, G., 2005. Vegetation fire in the savannas of the Llanos Orientales of Colombia. World Resour. Rev. 17 (4), 531–543.

Artaxo, P., Oliveira, P.H., Lara, L.L., Pauliquevis, T.M., Rizzo, L.V., Pires, C., Paixao, M.A., Longo, K.M., Freitas, S., Correia, A.L., 2006. Efeitos climaticos de partıculas de aerosoles biogenicos e emitidos em queimadas na Amazonia. Rev. Bras. Meteorol. 21 (3), 168–189.

Barnaba, F., Angelini, F., Curci, G., Gobbi, G.P., 2011. An important fingerprint of wildfires on the European aerosol load. Atmos. Chem. Phys. 11, 10487–10501.

Ben-Ami, Y., Koren, I., Rudich, Y., Artaxo, P., Martin, S.T., Andreae, M.O., 2010. Transport of North African dust from the Bodele depression to the Amazon Basin: a case study. Atmos. Chem. Phys. 10, 7533–7544.

Bevan, S.L., North, P.R.J., Grey, W.M.F., Los, S.O., Plummer, S.E., 2009. Impact of atmospheric aerosol from biomass burning on Amazon dry-season drought. J. Geophys. Res. 114, D09204. http://dx.doi.org/10.1029/2008JD011112.

Draxler, R.R., Hess, G.D., 1998. An overview of the HYSPLIT_4 modeling system of trajectories, dispersion, and deposition. Aust. Meteor. Mag. 47, 295–308.

Formenti, P., Andreae, M.O., Lange, L., Roberts, G., Cafmeyer, J., Rajta, I., Maenhaut, W., Holben, B.N., Artaxo, P., Lelieveld, J., 2001. Saharan dust in Brazil and Suriname during the Large-Scale Biosphere-Atmosphere Experiment in Amazonia (LBA)–Cooperative LBA Regional Experiment (CLAIRE) in March 1998. J. Geophys. Res. 106 (D14), 14,919–14,934.

Formenti, P., Rajot, J.L., Desboeufs, K., Caquineau, S., Chevaillier, S., Nava, S., Gaudichet, A., Journet, E., Triquet, S., Alfaro, S., Chiari, M., Haywood, J.M., Coe, H., Highwood, E.J., 2008. Regional variability of the composition of mineral dust from Western Africa: results from the AMMA SOP0/DABEX and DODO. J. Geophys. Res. 113, D00C13. http://dx.doi.org/10.1029/2008JD009903.

Forster, P., Ramaswamy, V., Artaxo, P., Berntsen, T., Betts, R., Fahey, D.W., Haywood, J., Lean, J., Lowe, D.C., Myhre, G., Nganga, J., Prinn, R., Raga, G., Schulz, M., Van Dorland, R., 2007. Changes in atmospheric constituents and in radiative forcing. In: Solomon, S., Qin, D., Manning, M., Chen, Z., Marquis, M., Averyt, K.B., Tignor, M., Miller, H.L. (Eds.), Climate Change 2007: The Physical Science Basis. Contribution of Working Group I to the Fourth Assessment Report of the Intergovernmental Panel on Climate Change. Cambridge University Press, Cambridge, United Kingdom and New York, NY, USA.

Freitas, S., Longo, K., Silva Dias, M.A.F., Silva Dias, P.L., Chatfield, R., Prins, E., Artaxo, P., Grell, G., Recuero, F., 2005. Monitoring the transport of biomass burning emissions in South America. Environ. Fluid Mech. 5, 135–167.

Giglio, L., Descloitres, J., Justice, C.O., Kaufman, Y., 2003. An enhanced contextual fire detection algorithm for MODIS. Remote Sens. Environ. 87, 273–282.

Giglio, L., Csiszar, I., Justice, C.O., 2006. Global distribution and seasonality of active fires as observed with the Terra and Aqua Moderate Resolution Imaging Spectroradiometer (MODIS) sensors. J. Geophys. Res. 111, G02016. http://dx.doi.org/10.1029/2005JG000142.

Hoelzemann, J.J., Longo, K.M., Fonseca, R.M., do Rosario, N.M.E., Elbern, H., Freitas, S.R., Pires, C., 2009. Regional representativity of AERONET observation sites during the biomass burning season in South America determined by correlation studies with MODIS Aerosol Optical Depth. J. Geophys. Res. 114, D13301. http://dx.doi.org/10.1029/2008JD010369.

Holben, B.N., et al., 1998. AERONET: a federated instrument network and data archive for aerosol characterization. Remote Sens. Environ. 66, 1–16.

Hubanks, P.A., King, M.D., Platnick, S., Pincus, R., 2008. MODIS Algorithm Theoretical Basis Document No. ATBD-MOD-30 for Level-3 Global Gridded Atmosphere Products.

Ichoku, C., Kaufman, Y.J., 2005. A method to derive smoke emission rates from MODIS fire radiative energy measurements. IEEE Trans. Geosci. Remote Sens. 43 (11), 2636–2649.

Ichoku, C., Giglio, L., Wooster, M.J., Remer, L.A., 2008. Global characterization of biomass-burning patterns using satellite measurements of fire radiative energy. Remote Sens. Environ. 112, 2950–2962.

Johnson, B.T., Osborne, S.R., Haywood, J.M., Harrison, M.A.J., 2008a. Aircraft measurements of biomass burning aerosol over West Africa during DABEX. J. Geophys. Res. 113, D00C12. http://dx.doi.org/10.1029/2008JD009848.

Johnson, B.T., Heese, B., McFarlane, S.A., Chazette, P., Jones, A., Bellouin, N., 2008b. Vertical distribution and radiative effects of mineral dust and biomass burning aerosol over West Africa during DABEX. J. Geophys. Res. 113, D00C12. http://dx.doi.org/10.1029/2008JD009848.

Justice, C., Giglio, L., Boschetti, L., Roy, D., Csiszar, I., Morisette, J., Kaufman, Y., 2006. Modis Fire Products. http://modis.gsfc.nasa.gov/data/atbd/atbd_mod14.pdf.

Kaufman, Y.J., Justice, C.O., Flynn, L.P., Kendall, J.D., Prins, E.M., Giglio, L., Ward, D.E., Menzel, W.P., Setzer, A.W., 1998. Potential global fire monitoring from EOS-MODIS. J. Geophys. Res. 103, 32215–32238.

Kaufman, Y.J., Koren, I., Remer, L.A., Tanre, D., Ginoux, P., Fan, S., 2005. Dust transport and deposition observed from the Terra-Moderate Resolution Imaging Spectroradiometer (MODIS) spacecraft over the Atlantic Ocean. J. Geophys. Res. 110, D10S12. http://dx.doi.org/10.1029/2003JD004436.

Koch, D., Bond, T.C., Streets, D., Unger, N., van der Werf, G.R., 2007. Global impacts of aerosols from particular regions and sectors. J. Geophys. Res. 112, D02205. http://dx.doi.org/10.1029/2005JD007024.

Koren, I., Kaufman, Y.J., Remer, L.A., Martins, J.V., 2004. Measurement of the effect of Amazon smoke on inhibition of cloud formation. Science 303 (5662), 1342–1345.

Koren, I., Kaufman, Y.J., Washington, R., Todd, M.C., Rudich, Y., Martins, J.V., Rosenfeld, D., 2006. The Bodélé depression: a single spot in the Sahara that provides most of the mineral dust to the Amazon forest. Environ. Res. Lett. 1 (014005). http://dx.doi.org/10.1088/1748-9326/1/1/014005.

Levy, R., Leptoukh, G., Kahn, R., Zubko, V., Gopalan, A., Remer, L., 2009. A critical look at deriving monthly aerosol optical depth from satellite data. IEEE Trans. Geosci. Remote Sens. 47 (9), 2942–2956.

Levy, R.C., Remer, L.A., Kleidman, R.G., Mattoo, S., Ichoku, C., Kahn, R., Eck, T.F., 2010. Global evaluation of the Collection 5 MODIS dark-target aerosol products over land. Atmos. Chem. Phys. 10, 10399–10420.

Longo, K.M., Freitas, S.R., Ulke, A.G., Hierro, R.F., 2006. Transport of biomass burning products in Southeastern South America and its relationship with the South American Low Level Jet East of the Andes. International Conference on Southern Hemisphere Meteorology and Oceanography (ICSHMO), 8, Foz do Iguaçu. Proceedings. INPE, São José dos Campos. ISBN: 85-17-00023-4, pp. 121–129 (CD-ROM).

Martin, S.T., et al., 2010. Sources and properties of Amazonian aerosol particles. Rev. Geophys. 48, RG2002. http://dx.doi.org/10.1029/2008RG000280.

Mielnicki, D.M., Canziani, P., Drummond, J., Skalanky, P., 2005. La quema de biomasa en Sudamérica vista desde el espacio. Anales IX Congreso Argentino de Meteorología. ISBN: 987-22411-0-4.

Mu, M., Randerson, J.T., van der Werf, G.R., Giglio, L., Kasibhatla, P., Morton, D., Collatz, G.J., DeFries, R.S., Hyer, E.J., Prins, E.M., Griffith, D.W.T., Wunch, D., Toon, G.C., Sherlock, V., Wennberg, P.O., 2011. Daily and 3-hourly variability in global fire emissions and consequences for atmospheric model predictions of carbon monoxide. J. Geophys. Res. 116, D24303. http://dx.doi.org/10.1029/2011JD016245.

Otero, L.O., Ristori, P.R., Quel, E.J., 2009. Fires, smoke and biomass burning across South America, August 23, 2006. AIP Conf. Proc. 1100, 311. http://dx.doi.org/10.1063/1.3116978.

Papastefanou, C., 2006. Residence time of tropospheric aerosols in association with radioactive nuclides. Appl. Radiat. Isot. 64, 93–100.

Pereira, G., Freitas, S.R., Moraes, E.C., Ferreira, N.J., Shimabukuro, Y., Rao, V., Longo, K.M., 2009. Estimating trace gas and aerosol emissions over South America: relationship between fire radiative energy released and aerosol optical depth observations. Atmos. Environ. 43, 6388–6397.

Prins, E.M., Feltz, J.M., Menzel, W.P., Ward, D.E., 1998. An overview of GOES-8 diurnal fire and smoke results for SCAR-B and 1995 fire season in South America. J. Geophys. Res. 103 (D24), 31,821–31,835. http://dx.doi.org/10.1029/98JD01720.

Procopio, A.S., Artaxo, P., Kaufman, Y.J., Remer, L.A., Schafer, J.S., Holben, B.N., 2004. Multiyear analysis of Amazonian biomass burning smoke radiative forcing of climate. Geophys. Res. Lett. 31, L03108. http://dx.doi.org/10.1029/2003GL018646.

Reid, J.S., Eck, T.F., Christopher, S.A., Koppmann, R., Dubovik, O., Eleuterio, D.P., Holben, B.N., Reid, E.A., Zhang, J., 2005. A review of biomass burning emissions part III: intensive optical properties of biomass burningparticles. Atmos. Chem. Phys. 5, 827–849.

Roberts, G., Wooster, M.J., Lagoudakis, E., 2009. Annual and diurnal African biomass burning temporal dynamics. Biogeosciences 6, 849–866.

Schafer, J.S., Eck, T.F., Holben, B.N., Artaxo, P., Duarte, A.F., 2008. Characterization of the optical properties of atmospheric aerosols in Amazonia from long-term AERONET monitoring (1993–1995 and 1999–2006). J. Geophys. Res. 113, D04204. http://dx.doi.org/10.1029/2007JD009319.

Ten Hoeve, J.E., Remer, L.A., Correia, A.L., Jacobson, M.Z., 2012. Recent shift from forest to savanna burning in the Amazon Basin observed by satellite. Environ. Res. Lett. 7, 024020. http://dx.doi.org/10.1088/1748-9326/7/2/024020.

Wooster, M.J., Roberts, G., Perry, G.L.W., 2005. Retrieval of biomass combustion rates and totals from fire radiative power observations: FRP derivation and calibration relationships between biomass consumption and fire radiative energy release. J. Geophys. Res. 110, D24311. http://dx.doi.org/10.1029/2005JD006318.